



Production cost modeling for permanent magnet synchronous machines for electric vehicles

Jonas Hemsen¹ · Nikita Nowak¹ · Lutz Eckstein¹

Received: 17 January 2023 / Accepted: 10 March 2023 / Published online: 18 April 2023
© The Author(s) 2023

Abstract

A cost model for the estimation of production costs of permanent magnet synchronous machines (PMSM) is presented, which allows to alter design choices such as wire technology, winding layout, cooling system, materials and more. With the goal to make results reproducible by others, the methods are explained in detail and used data and assumptions are given. The developed model helps to understand the interaction between the design of PMSM, manufacturing methods and the resulting costs. With it, different PMSM technologies and materials can be evaluated regarding its influence on the production costs, which is a prerequisite to find the best compromise between performance and costs. Production volume is shown to be the most decisive factor for the resulting production costs. Between minimum and maximum assumed volumes, an average cost per unit reduction of 67% could be observed. Furthermore, the results imply that the winding production is responsible for the greatest part of the overall costs, followed by the rotor assembly (including rare earth magnets). When using the model to compare different wire types, it can be stated that up to a production volume of roughly 150,000 units/year, hairpin wires are more expensive to produce. Above this volume, hairpin windings will get cheaper than round wire windings due to its higher grade of automation of the production process. Through the conducted investigations and the presented results, it is demonstrated that the cost model can serve to evaluate technologies with regards to costs in the early development stage. This way a more holistic assessment of technologies for PMSM is possible, helping to find the ideal compromises between costs and performance and to increase the attractiveness of sustainable mobility.

Keywords Cost modeling · Electric vehicles · Permanent magnet synchronous motor · Production costs

1 Introduction

Climate change is omnipresent and it is one of the greatest crises of mankind. One way to fight it is to lower anthropogenic greenhouse gas emissions by road transport, which is responsible for 21% of overall emissions [17]. Due to the fact that battery-electric vehicles (BEV) emit up to 70% less greenhouse gases over their lifetime compared to conventional combustion vehicles [46], more electric vehicles on the road can significantly contribute to fighting climate change. Currently however, the contribution is low, at the end of 2021 only

0.9% of all vehicles on the road in Europe were battery-electric [14]. To further increase the number of registrations and the share of BEV on the road, the electric versions of vehicle models must be competitive in terms of purchase price, which is not the case nowadays. It is hence of crucial importance during the development of novel drivetrain technologies to not only evaluate performance of an innovation but also its costs. To do so, sophisticated and flexible cost models of the drivetrain components are required.

Unfortunately, no adequate cost model for this intention could be found during a literature study (cf. chapter 2) so that an own model had to be invented. Accordingly, in this research article, the developed high-fidelity production cost model is presented that serves to evaluate production costs of permanent magnet motors (currently the most used motor type in BEV) in the early design stage. The effect of design decisions (e.g. winding type, coil configuration, cooling system, etc.) on the resulting production costs can be directly evaluated. This way, the motor technologies can be chosen, which provide the ideal compromise between performance

✉ Jonas Hemsen
jonas.hemsen@ika.rwth-aachen.de
Nikita Nowak
nikita.nowak@rwth-aachen.de
Lutz Eckstein
lutz.eckstein@ika.rwth-aachen.de

¹ Institute for Automotive Engineering (ika), RWTH Aachen University, Aachen, Germany

and production costs. Hence, this model can contribute to make EV more affordable and more attractive to customers and to increase their sales.

The article is structured in the following way: Chapter 2 provides an overview of the most actual research activities in the topic of production cost models for electric motors. Chapter 3 contains the detailed methodological overview of the developed production cost model. The validation of the presented methods with the help of results from other public research is then presented in chapter 4. The following chapter 5 presents results of the developed model with 16 reference electric machines (EM) and exemplary technology variation of winding type and cooling system. The research is summarized and concluded in chapter 6.

2 Literature review

Initially, a literature review is presented to understand the current research status and to emphasize the need for a novel public high-fidelity cost model for PMSM.

Bubert [8] developed a simple cost model for PMSM that computes costs based on power requirement and production volume. Production costs are determined by a fixed factor on material costs. The factors are determined with data from [26], allowing a scaling of costs with production volume. However, since individual production steps are disregarded, the impact of design changes on costs cannot be evaluated [36]. Consequently, no technology and material variation can be included in this model. Also, the model scales the costs almost linearly with power, which is not valid according to other researchers [18, 33, 37].

Propfe [37] goes more into the detail of the electric motor production processes. A fixed sequence of manufacturing processes is assumed for each machine type. The costs are calculated for each step and added to material and energy costs. Unfortunately, the authors do not present the used equations. Furthermore, a scaling method for machine costs with production volume is missing. Since the production process is fixed here, the model does not allow for a variation of cooling system or wire type.

Fyhr [18] also considers the electric motor production steps. He provides general equations for a cost model based on the accumulation of individual production step cost. Costs for a production step contain investment costs, cost of the capital, tooling and fixture costs. He also states the assumed production steps for a PMSM and discusses them in detail. However, using the presented equations is difficult due to a lack of information: Equations are only given in general form and no information of the parametrization of its coefficients with help of the machine design parameters is given.

As a conclusion, no detailed enough and fully published cost model could be found in literature that serves the intention of evaluating technology, material and production volume changes. This may also have to do with the fact, that cost engineering is typically more intensively performed from companies in the private sector, which like to keep their intellectual property about production costs unpublished.

3 Methodology

To calculate its production costs K_{EM} , the electric motor is split up into housing, magnets, windings, sheet stack, shaft, and cooling system. For each of the six parts p , the model estimates the calculated costs originating from the manufacturing processes K_{manu} , (cf. Sects. 3.1 and 3.2) the used materials K_{mat} (cf. Sect. 3.3) and the labor K_{lab} (cf. Sect. 3.4). Additional positions, contributing to the overall production costs are the parts that are typically purchased from suppliers K_{purch} (cf. Sect. 3.5) as well as the final assembly process K_{ass} (cf. Sect. 3.6).

$$K_{EM} = \left(\sum_{p=1}^{\#parts} K_{manu,p} + K_{mat,p} + K_{lab,p} \right) + K_{purch} + K_{ass}$$

3.1 Manufacturing costs

Due to the machine-intensive production, the *machine hour rate calculation* is a suitable manufacturing cost model type [36]. Every used production machine represents a separate cost center so that the overall costs $K_{manu,p}$ for one EM are the sum of the individual manufacturing step costs:

$$K_{manu,p} = \sum_{i=1}^{\#steps} K_{Mh,i} t_i$$

For every production machine and thereby for every cost center a machine hour rate $K_{Mh,i}$ is calculated: it describes the costs per hour caused by a production step. The absolute costs for the production step for one EM are then the product of its machine hour rate $K_{Mh,i}$ and its cycle time t_i . The machine hour rate is composed of the depreciation charges $K_{D,i}$, imputed interest costs $K_{I,i}$, costs of space $K_{S,i}$, energy costs $K_{E,i}$, and maintenance costs $K_{M,i}$. In addition to the depreciation charges which cover the investment costs of the production, machine tooling costs $K_{T,i}$ need to be considered [36]. The machine hour rate is thus calculated as follows:

$$K_{Mh,i} = K_{D,i} + K_{I,i} + K_{S,i} + K_{E,i} + K_{M,i} + K_{T,i}$$

To apply the machine hour rate calculation to a production line with multiple machines and various cycle times of the

production steps, it is important to calculate the number of production machines N_i and the needed runtime of these for a given yearly output of EMs. For every production step i , the number of production machines n_i can be derived by the cycle time t_i , the production volume X and the maximal yearly production hours T :

$$n_i = \frac{Xt_i}{T}$$

In the rare case that $n_i \in \mathbb{N}$, the production machine(s) would run at maximum capacity. But in most cases n_i is a decimal number so that it takes $\lfloor n_i \rfloor$ production machines producing at a yearly runtime T and another additional machine producing at a fraction of T to reach the desired production volume X . The fractional runtime $T_{frac,i}$ of the additional machine can be calculated to:

$$T_{frac,i} = T (n_i - \lfloor n_i \rfloor)$$

With the presented formulas, the machine hour rate calculation can be modified to fit a production line with multiple production machines, as seen in the following. The shown equations assume that $T_{frac,i} \neq 0$. For the rare case of $T_{frac,i} = 0$ the equations need to be adapted so that $\frac{1}{T_{frac,i}}$ is no longer considered.

The depreciation charges $K_{D,i}$ cover the yearly imputed depreciation. For simplification, linear depreciation is chosen. The machine's investment cost C_i gets distributed equally over its period of use. The period of use D_i for the different production machines is defined by the federal ministry (see Table 12). The depreciation charges $K_{D,i}$ are calculated to:

$$K_{D,i} = \frac{C_i}{D_i} \left(\frac{\lfloor n_i \rfloor}{T} + \frac{1}{T_{frac,i}} \right)$$

The interest costs $K_{I,i}$ represent an imputed loss because of the tied-up capital in the machine. On average, half of the machine's investment cost C_i are bound throughout the period of use D_i . The imputed interest rate I for 2022, here determined by the Municipal Audit Office North Rhine-Westphalia, is 5.242%. This leads to interest costs in the amount of:

$$K_{I,i} = \frac{C_i}{2} I \left(\frac{\lfloor n_i \rfloor}{T} + \frac{1}{T_{frac,i}} \right)$$

Costs of space $K_{S,i}$ distribute the rental costs for the production halls to the production machines. Basis of the calculation are the needed space for the machine S_i and the yearly rental costs per square meter K_{qm} (cf. Table 11):

$$K_{S,i} = S_i K_{qm} \left(\frac{\lfloor n_i \rfloor}{T} + \frac{1}{T_{frac,i}} \right)$$

To consider the machine's use of electricity energy costs $K_{E,i}$ are introduced using the yearly energy consumption E_i and the costs of electricity k_E :

$$K_{E,i} = E_i k_E \left(\frac{\lfloor n_i \rfloor}{T} + \frac{1}{T_{frac,i}} \right)$$

Because of high usage rates of the machines and a resulting need of service, maintenance costs $K_{M,i}$ are added to the machine hour rate calculation. This is done with a factor z_M on the machine's depreciation charges $K_{D,i}$:

$$K_{M,i} = z_M K_{D,i}$$

The same method with a factor z_T is used to calculate the tool costs $K_{T,i}$ of a production machine. These costs represent e.g., a drilling head that wears out.

$$K_{T,i} = C_i z_T \left(\frac{\lfloor n_i \rfloor}{T} + \frac{1}{T_{frac,i}} \right)$$

Note: Due to of the possible case that $\frac{1}{T_{frac,i}} \rightarrow \infty$, the production costs can reach peaks at unknown production volumes. These are only theoretical artifacts which are not considered here for practical purposes.

3.2 Manufacturing processes

In the following, the production processes for the parts housing, sheets, magnets, windings, and shaft as well as for the four considered cooling systems frame, winding, end winding, and rotor cooling are described. For a better understanding, the described production machines are consecutively numbered (#1 to #24) and its used parameters are listed in the appendix in Table 12.

3.2.1 Housing

The production process for the electrical machine's housing is split into the processes of die casting (#1), machining (#2), deburring (#3), and pressure blasting (#4).

During die casting (#1), the raw material is melted and injected into a form. The needed raw aluminum is calculated through the estimated volume of the housing $V_{Housing}$:

$$m_{housing} = \rho_{aluminum} V_{housing}$$

The standard cycle time of the die casting process is set to two minutes with a correction factor for different housing volumes. The correction factor accounts for the fact that the cycle time (and accordingly the operating costs) of the

casting machine get higher with increased volume of the mold [18]:

$$t_1 = 120s \frac{V_{housing}}{0.45}$$

After cooling down, the product needs further machining processes. Firstly, a cycle time of 120 s is assumed for the machining center. A surcharge of 5% considers the complexity of a housing in comparison to standard die casting products.

$$t_2 = 126s$$

In the next step, the housing needs to undergo a deburring process. A cycle time of 60 s per housing is assumed.

$$t_3 = 60s$$

In a last step, the housing gets cleaned by a pressure blasting system. It is assumed that nine housings can be processed by the machine per minute.

$$t_4 = 6.7s$$

3.2.2 Sheets

Rotor and stator of electric machines consist of many single electrical sheets glued together. The production of the sheets is split into two processes. First, the desired form for the rotor and stator needs to be punch pressed (#5) from the raw electrical sheet material. The number of needed single iron sheets can be calculated by the length of stator/rotor l_{stack} , the thickness of a single iron sheet d_{sheet} , and the iron fill factor of the stack k_{stack} :

$$n_{Sheets} = \frac{l_{stack}k_{Stack}}{d_{Sheet}}$$

In large-scale production punch press machines can reach 150 strokes per min [26] resulting in a cycle time per electric machine of:

$$t_5 = 0.4sn_{Sheets}$$

Table 1 Punch press tooling costs increase depending on the sheet diameter

Sheet diameter d [m]	Increase in tooling costs (%)
$d \leq 0.1$	0
$0.1 < d \leq 0.2$	20
$0.2 < d \leq 0.3$	35
$d > 0.3$	50

Furthermore, the tooling costs for the punch press machine are assumed to increase with the diameter of the sheets and the number of slots due to more wear (Tables 1, 2).

In general, the material needed for the stator and rotor sheets is calculated by the masses of the components $m_{sheets,stator}$ and $m_{sheets,rotor}$. Those can be estimated using analytical approaches, or (as here) are part of the FEM calculation results. Furthermore, the masses are multiplied with a dynamic factor k_{sheets} , which considers the waste material due to punching.

$$m_{sheets} = (m_{sheets,stator} + m_{sheets,rotor})(1 + k_{sheets})$$

In the next step, the pressed iron sheets need to be pack-etized and glued together to form the basis of the stator or rotor. A machine (#6), combining the process steps of pack-etizing and gluing the sheets is considered. The cycle time adds up to 305 s for the sheets of stator and rotor:

$$t_6 = 305s$$

3.2.3 Magnets

The magnets for the rotor of the PMSM need to be inserted into the slots of the rotor sheet. In this model, it is assumed that the magnets are acquired from a supplier and thus the magnets are included as material costs (cf. Sect. 3.3). Above a certain size of the magnets of approximately 30 g the magnets need to be inserted into the rotor cavities by an automatic robotic system (#7). The cycle time t_7 used in this model is estimated by the absolute costs for the magnet assembly in a large production environment [26]:

$$t_7 = 295s$$

3.2.4 Windings

To cover a wide range of possible layouts of PMSM, the stator windings can be chosen between round wires, hairpins or Formed-Litz wire. Furthermore, the winding layout of the

Table 2 Punch press tooling costs depending on the number of slots

Number of slots n_{slots}	Increase in tooling costs (%)
$n_{slots} \leq 12$	0
$12 < n_{slots} \leq 24$	15
$24 < n_{slots} \leq 36$	30
$36 < n_{slots} \leq 48$	45
$48 < n_{slots} \leq 84$	60
$n_{slots} > 84$	75

electrical machine can be specified by the number of winding layers, wires per slot, strands in hand, and coil span. Independent from the selected winding type there are a few production steps that are always necessary for the windings.

In the first step, the slots of the stator need to be isolated so that there are no power flashovers between the copper windings and the iron sheets of the stator. This is achieved by inserting insulation paper in every slot of the stator. The needed amount of paper is calculated by the number of slots n_{slots} , the stack length l_{stack} , and the circumference U_{slot} of the slot:

$$A_{Paper} = n_{slots} (l_{stack} + 0.01m) U_{slot}$$

On both ends of the stator, an overhang of the insulation paper of 5 mm each is assumed. Furthermore, the amount of needed paper increases if the slot contains strands of two phases (two-layer windings) due to the required phase insulation in the middle of a slot. Then the needed amount of paper A_{Paper} increases by $A_{Paper,phase}$:

$$A_{Paper,phase} = n_{slots} (l_{stack} + 0.01m) w_{slot}$$

The parameter w_{slot} describes the width of the slot in its radial middle.

With distributed round windings, an additional need for phase insulation arises at the winding heads since the different phases lay on top of each other. The surface area of the winding heads can be calculated by the height of the end windings h_{enwi} and the length of the passive stator windings $l_{passive}$. It is assumed that 50% of the phase winding needs to be covered with insulation paper.

$$A_{enwi} = 0.5\pi h_{enwi} l_{passive}$$

The needed amount of insulation paper for both sides of the stator is then calculated in dependence on the number of phases n_{phases} :

$$A_{enwi,paper} = 2A_{enwi} \frac{n_{phases} - 1}{2}$$

For the closing of the slot towards the air gap, cover slides are used. Independent from slot geometry, it is assumed that they have a fixed width of 11 mm with a horizontal overhang of 2 mm per side. Again, an axial overhang of 5 mm on both ends of the stator is assumed. The needed length of the cover slides can be calculated to:

$$l_{Slides} = n_{slots} (l_{stack} + 0.01m)$$

The machines inserting the insulation paper using pressure (#8) have a cycle time of [1]:

$$t_8 = 1.5sn_{insertions}$$

It is assumed that the insertion of the cover slides can be fulfilled with the same system and the same cycle time. The number of insertions $n_{insertions}$ adds up to:

$$N_{insertions} = \begin{cases} 2n_{slots}, one - layerwindings \\ 3n_{slots}, two - layerwindings \end{cases}$$

After the insulation paper was inserted, the windings can be placed in the slots. These processes are described in the following Sects. 3.2.4.1 to 3.2.4.3. The stator production ends, for all possible winding types with the impregnation (#9) of the windings.

The needed amount of impregnation resin V_{resin} is calculated by the free space in the slot volume, which is not covered by copper wires. For simplification, it is assumed that the slot cavities are fully filled with resin but no resin at the winding head is considered.

$$V_{resin} = V_{slot}(1 - k_{copper})$$

V_{slot} is the available volume in the slot and k_{copper} is the copper fill factor in the slot.

3.2.4.1 Round wire The production of stators with classical round wires can be done by various processes. In Hagedorn and Blanc [21] the linear, needle, and flyer winding, as well as the insertion technique are presented as production processes for automotive applications. The linear winding technique can only be used for concentrated windings, so it does not fit the requirements of most PMSM. The needle winding method on the other hand can produce both concentrated and distributed windings. Nevertheless, the insertion winding technique for distributed windings is additionally implemented in the model because of the high relevance in the automotive industry.

For the needle winding process, machines (#10) from Aumann AG are used. It is assumed that the winding speed is linearly dependent on the wire length of one turn. The machine's maximum winding speed is at 450 windings per minute while for the minimum winding speed, 120 windings per minute are stated [4]. As possible wire lengths (one turn) a range from 100 to 720 mm is common. Assuming that with the shortest wire length, 450 windings per minute and with the longest wire length 120 windings per minute are possible, the following equation can be set up, interpolating the winding speed v_{wind} in turns per second in dependence of the wire length per turn l_{turn} in meters:

$$v_{wind} = 8.39 \frac{1}{s} - 8.87 \frac{1}{sm} l_{turn}$$

Because of the chosen machine with two spindles the cycle time can be halved as two stators at the same time

can be processed. Furthermore, the cycle time for the stator windings is extended by a setup time of 10 s [21] and approximately 4 s for every new coil that needs to be wound [5]. As mentioned before the needle winding technique can be used for concentrated and as well distributed windings. Nevertheless, the production process for distributed windings is slightly different as so-called winding tools are needed. Using a needle winding machine for this type of winding design results in covering the slots in between a coil with the copper winding because of the trajectory of the needle. In [44] this problem is furtherly described with possible solutions. The mentioned winding tools have prevailed so that this model resorts to this technique. These tools are used to cover the problematic slots and build space so that the windings can be placed over the stator teeth. After the coil is wound, the tools can be removed and the slots in between the coil are still accessible to wind the other coils. Due to the current lack of practical use of these tools the production process needed to be assumed. In general, the number of required winding tools corresponds to twice the number of poles p . In this model it is assumed that the winding tools need to be moved manually after the winding of every phase. For this process step ten seconds of time consumption are calculated. It is depending on number of phases n_{phases} and the number of winding tools ($2p$), resulting in a cycle time increase of:

$$t_{windingtools} = 10s2pn_{phases}$$

The overall cycle time for the needle winding machine then results as the sum of the actual winding process and tool arrangement:

$$t_{10} = t_{windingtools} + \frac{n_{turnspercoil}}{v_{wind}}$$

For a needle winding machine there is an average need of 0.5 employees [23].

For the flyer winding process a machine (#11) from Aumann AG is chosen. This machine also has two spindles but can reach a winding speed of 50 windings per second. For the manual loading and unloading of the wound coils at the flyer machine five seconds are assumed each time resulting in a total cycle time of:

$$t_{11} = 10sn_{coils} + \frac{n_{turnspercoil}n_{coils}}{50}s$$

Because of similarities to the needle winding machine again 0.5 employees per machine are assumed.

Like mentioned above, the flyer winding technique can be used for concentrated windings or with an additional insertion machine (#12) for distributed windings. This machine inserts the previously wound coils of one phase into the

stator. The cycle time according to Hagedorn and Blanc [21] adds up to approximately:

$$t_{12} = 9sn_{phases}$$

In a next step, the single copper wires are contacted. The number of welding points is dependent on the number of parallel coils $n_{coils,||}$ and the number of parallel wires in each coil $n_{wires,||}$ also often called “strands in hand”. The total number of welding points can be calculated to:

$$n_{welding,total} = n_{welding,coils} + n_{welding,strands}$$

With:

$$n_{welding,coils} = \begin{cases} 0, & n_{coils,||} \leq 1 \\ 2n_{phases}, & n_{coils,||} > 1 \end{cases}$$

$$n_{welding,strands} = \begin{cases} 0, & n_{wires,||} \leq 1 \\ 2n_{phases} \cdot n_{wires,||}, & n_{wires,||} > 1 \end{cases}$$

The machine used for the welding process is a laser welding machine (#13). According to [19] such machines are normally used for the welding of hairpin bars. But herein, it is assumed that the machines can also be used for contacting the parallel wires of the windings. A laser welding machine uses image processing to identify the exact positions of the welding points. After four seconds of setup time and 20 s of image processing, the production machine needs 0.22 s per welding point and 2.4 ms to jump to the next welding point. The cycle thus results to:

$$t_{13a} = 24s + 0.2224sn_{welding,total}$$

In a further step it is necessary to contact the phases of the windings to the terminal as well as creating the star point. For this purpose, first the copper bundles of the phases are manually inserted into winding sleeves. A worker needs approximately 15 s per sleeve [1] resulting in a cycle time of:

$$t_{sleeves} = 15sn_{sleeves}$$

The number of winding sleeves $n_{sleeves}$ can be calculated to:

$$n_{sleeves} = 2n_{phases}n_{layers}$$

Each sleeve is assumed to have 0.5 m of length. The costs per meter of sleeve material are stated in Table 5.

Then the copper bundles can be contacted to the terminal and the star point can be created. Therefore, the ultrasonic technique (#14) is selected. The number of welding points $n_{welding,terminal}$ adds up to:

$$n_{welding,terminal} = n_{phases} + n_{starpoints}$$

The number of star points of the winding $n_{starpoints}$ usually equals one, it may however vary for machines with other than three phases (e.g. a 2×3 phase winding).

The ultrasonic welding machine needs four seconds to setup and 1.4 s for the welding process as well as 1.2 s for jumping to the next welding point resulting in a cycle time of:

$$t_{14} = 4s + 3.6sn_{weldingpoints}$$

The last step is the bandaging of the winding heads. The cycle time per stator of the bandaging machine (#15) is assumed to:

$$t_{15} = 180s$$

3.2.4.2 Hairpins In the first step of the production of a hairpin stator, the copper bar material needs to be processed into the single hairpins. It is assumed that the raw material for the hairpins already has an insulation layer. Thereby material costs of 5.80 €/kg additional to the material price of raw copper are assumed for hairpins. A machine (#16) of the company Otto Bihler Maschinenfabrik GmbH & Co. KG combines the process steps of setting, cutting, and stripping the raw copper bars and forming them into hairpins. According to the manufacturer the machine needs three to ten minutes of setup time per stator variant which can then produce 80 hairpins per minute. With the number of hairpins $n_{Hairpins}$ the cycle time results in:

$$t_{16} = 0.75sn_{hairpins}$$

In a further step the hairpins are preassembled to a basket. The used production machine (#17) needs approximated 0.8 s per hairpin to set it. The cycle time can be calculated to:

$$t_{17} = 0.8sn_{hairpins}$$

The amount of hairpin baskets is dependent on the number of winding layers n_{Layers} and the hairpins per slot $n_{Hairpins,slot}$:

$$n_{baskets} = \frac{n_{layers}n_{hairpins,slot}}{2}$$

The next production machine (#18) inserts the hairpin baskets into the slots of the stator. It needs approximately 25 s for one hairpin basket resulting in:

$$t_{18} = 25sn_{baskets}$$

To allow the twisting of hairpins the copper ends of them need to be necked creating a space between the ends of the hairpins. This production machine (#19) requires 20 s per stator. The cycle time thereby is fixed to:

$$t_{19} = 20s$$

Like mentioned before, the copper ends need to be twisted so that the hairpins can be connected and form a circuit. In two steps of 20 s each, a production machine (#20) performs the work, resulting in a parameter-independent cycle time of:

$$t_{20} = 40s$$

The last step of the individual hairpin stator production process is the welding of the twisted hairpin ends. Because of the findings from [19], the same laser welding machine as for the coil and strand connection is chosen (#13). The amount of welding points $n_{welding,hp}$ is calculated with the number of hairpins $n_{hairpins}$ and the number of phases n_{Phases} to:

$$n_{welding,hp} = n_{hairpins}n_{phases}$$

Thus, the cycle time is:

$$t_{13b} = 24s + 0.2224sn_{welding,hp}$$

3.2.4.3 Formed-Litz wire Formed-Litz wire is a form-pressed round wire, which increases the copper density in the wire and consequently the fill factor to between 60 and 70%. These wires are often produced with thermal bonding wire, meaning that through heating the wire gets stiff, comparably to a hairpin bar [40]. It is therefore assumed in this model, that windings using Formed-Litz wire are produced with the same production processes than hairpin windings. This has been described in Sect. 3.2.4.2 before.

As a material price for FLW 11.20 €/kg additional to the material price of raw copper (cf. Table 5) is assumed [45].

3.2.5 Shaft

The production of the shaft is split into four steps. In a first step the raw material (hardened steel) is cut by the length of the shaft. Appropriate machines (#21) can handle 50 shafts per minute resulting in a cycle time of:

$$t_{21} = 1.2s$$

The shaping of the shaft is done at a lathe machine (#22). The machining velocity v_C , the feed f and the back engagement of cutting edge a_p are material and machine dependent. The values are listed in Table 3 below:

The cycle time for the lathe for one shaft segment can be calculated using the parameters from Table 3 and the raw material diameter d_{raw} , the length of the segment $l_{shaft,s}$ and the desired diameter $d_{final,s}$. The overall cycle time is the sum of the cycle times of each shaft segment s .

Table 3 Parameters for the lathe machine [47]

Parameter	Value
v_C	2.5 m/s
f	$7 * 10^{-4}$ m/turn
a_p	$2.5 * 10^{-3}$ m

$$t_{22} = \sum_{s=1}^{\#segments} \frac{\pi d_{raw} l_{shaft,s} (d_{raw} - d_{final,s})}{v_C f a_p}$$

With the presented formula for the cycle time of the lathe machine, the shape of the shaft can be considered with different lengths and diameters. Here however, a relatively simple shaft geometry is considered: The shaft has the radius identical to the inner rotor radius over the sheet stack length and two equal parts with reduced radius at each side (Fig. 1).

After the shaping of the shaft is done it needs further processing at a machining center (#23). For the model it is assumed that this process step can handle one shaft per minute resulting in a cycle time of:

$$t_{23} = 60s$$

The last step of the production of the electrical machine’s shaft is the induction hardening. The shaft is heated and immediately quickly quenched so that the material gets harder. An induction hardening machine (#24) has a cycle time according to [7, 26] of:

$$t_{24} = 20s$$

3.2.6 Cooling system

Electric motors in automotive applications are always liquid cooled due to the requirements of high compactness and low weight [9]. Commonly seen cooling systems comprise water jacket cooling (e.g. VW electric motors and Jaguar I-Pace), direct winding cooling with oil (e.g. Tesla) and rotor shaft cooling (e.g. Audi e-tron). Within this model, four different cooling systems can be evaluated regarding its production costs: Frame cooling (Sect. 3.2.6.1), end-winding cooling (Sect. 3.2.6.2), full-winding cooling (Sect. 3.2.6.3) and rotor

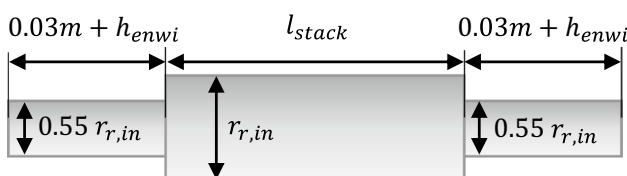


Fig. 1 Assumed shaft geometry (3 segments)

cooling (Sect. 3.2.6.4). Independent of the selected cooling system and production volume, costs occur for the generally required parts for such a system (Table 4).

All the cooling systems presented in this chapter are realized through the adaption of existing parts of the electrical machine. This way, the production processes from previous chapters are used.

3.2.6.1 Frame cooling The frame cooling is the most common cooling system among the presented possibilities. In this model the frame cooling design is similar as presented in [20], where the housing of the electrical machine has spiral channels. To reduce production costs, it is estimated that these channels can be created in the housing casting process step described in Sect. 3.2.1 so that the form that is used for the die casting features the cooling channels. This requires a second outer housing in a cylindrical form that closes the cooling channel in radial direction. An example of this outer housing can be found in Kampker [24].

Because of the chosen production process (casting), a frame cooling system can save some material of the housing because of the hollow cooling channels. The volume of these spirally arranged channels V_{ch} can be calculated to:

$$V_{ch} = \sqrt{l_s^2 + \left(2\pi \frac{l_s}{w_{ch} + 0.01m} (r_{M,in} + l_{M,in})\right)^2} w_{ch} h_{ch}$$

Here, w_{ch} describes the width of the channel, h_{ch} the channel height and $r_{M,in}$ the stator radius. The radial distance between the cooling channel and the inner side of the housing $l_{M,in}$ is set to 3 mm [20]. The material savings m_{ch} from the cooling channel can then be calculated to:

$$m_{ch} = \rho_{aluminum} V_{ch}$$

3.2.6.2 End winding cooling In this model an end-winding cooling system is introduced, which uses two toroidal housings for the winding heads (cf. [38]). The mentioned housings follow the same production process as the main housing described in Sect. 3.2.1 except for using different parameters for the size and surface quality. In this model the housings for the winding heads are represented by a torus with rectangular cross section. The needed raw material volume for these hous-

Table 4 Purchased parts for the general cooling system

Part	Price [€]	Reference
Coolant pump	30.60	[30]
NTC	1.88	[25]
Sealing cord	3.53 /m	[39]

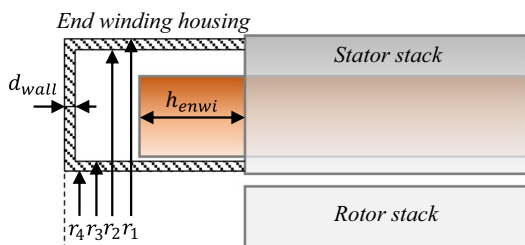


Fig. 2 Dimensions on the assumed end-winding housing

Table 5 Prices for standard materials

Material	Price	Reference
Copper	7.79 €/kg	[12]
Steel 16MnCr5	1.02 €/kg	[16]
Aluminum	2.42 €/kg	[11]
Insulation paper	26.60 €/m ²	[39]
Cover slide	0.42 €/m	[32]
Sleeve	0.50 €/m	[31]
Resin	10.00 €/dm ³	[13]

ings V_{cap} is calculated by following equation with the parameters displayed in Fig. 2.

$$V_{cap} = 2\pi h_{enwi} \left(r_1^2 \left(1 + \frac{d_{wall}}{h_{enwi}} \right) - r_2^2 + r_3^2 - r_4^2 \left(1 + \frac{d_{wall}}{h_{enwi}} \right) \right)$$

Additionally to the two housings, a sealing cord is needed between the housing’s walls and the stator stack. Two sealing locations for each of the two housings are needed resulting in a sealing cord length of:

$$l_{sealing} = 4\pi(r_1 + r_2 + r_3 + r_4)$$

3.2.6.3 Full winding cooling The full-winding cooling system is based on the end-winding cooling system and its winding head housings. Additionally, a sealing, respectively, cover slides between active winding and the air gap are required to prevent the cooling liquid from getting in contact with the rotor. With this system the active windings are directly cooled as shown in [41] and [34]. It is assumed that the cover slides must be inserted manually into the stator slots. The cycle time is estimated to:

$$t_{fullwindingcooling} = 10sn_{slots}$$

It shall be noted here, that in comparison to the end-winding cooling additional space between the wires is required for the coolant path and that therefore, the copper fill factor is considered lower, resulting in less overall copper material being used for the full-winding cooling.

3.2.6.4 Rotor cooling The rotor or shaft cooling represents another popular cooling system to increase the magnet cooling capabilities. For this model, the layout of the rotor cooling is based on that of the Audi e-tron [2]. The shaft is made hollow by drilling and an aluminum pipe is inserted into the shaft. The pipe forms the inlet for the coolant. The machining center used in the production process of the shaft can also be used to perform the drilling. The cycle time for the drilling is depending on the diameter d_{drill} that needs to be drilled out, the length of the drilling l_{drill} and the parameters v_c and f presented in Table 3.

$$t_{drill} = \frac{\pi d_{drill} l_{drill}}{v_c f}$$

It is assumed that to provide the rotor cooling, 90% of the shaft’s length needs to be drilled out and 65% of the shaft’s diameter. Furthermore, the length of the needed pipe is set to 90% of the drilling depth. The costs for a suitable aluminum pipe are estimated independent from the bore diameter. An average price of 6.39 € per meter can be assumed [29].

3.3 Material costs

3.3.1 Material prices

To allow the cost calculation of many different PMSM designs, it is crucial to consider different materials for the EM’s parts. The materials are separated into two groups. Raw materials (copper, steel, and aluminum) as well as purchased materials are assumed as “static”. The costs for those are calculated by the price per weight/length/area/volume (Table 5).

On the other hand, we consider materials whose price is scaled by their characteristics: Iron sheets and rare earth magnets. The price of the iron sheets used for the stator and rotor is assumed to be dependent on the thickness of a single sheet. Selecting thinner iron sheets results in higher costs for the same amount of material but also in lower eddy current losses. Based on an internal study the prices for different iron sheet materials are approximated by an

exponential relation. With a price of 1 €/kg for an iron sheet with a thickness of 0.35 mm the prices for other iron sheets with a thickness d (in mm) can be derived:

$$K = \frac{1 \frac{\text{€}}{\text{kg}} \cdot 0.35 \text{ mm}}{d}$$

The price for different magnet materials is assumed to be dependent on its grade, more specifically on the maximum energy product \hat{E} of the selected magnet. It is defined as the maximum product of the magnetic flux density B and the magnetic field strength H along the demagnetization curve of a magnetic material in second quadrant of the BH-curve. Based on a price of 66.45 €/kg for N38 magnet with a max. energy product of 38 MGOe the price of every magnet material with a certain max. energy product \hat{E} can be approximated by:

$$K_{\text{Magnet}} = \hat{E} \frac{66.45 \frac{\text{€}}{\text{kg}}}{38 \text{ MGOe}}$$

In the choice of the type of insulation paper for the stator windings, the thermal class plays a crucial role. Here, insulation paper with the thermal class H is selected to assure a temperature limit of 180 °C. Specifically, we chose TRIV-OLTHERM® NKN paper with a thickness of 0.2 mm and a price of 141 €/kg or 26.60 €/m² [28, 39].

The selected slot cover slides also fulfill the thermal class H and cause costs of 0.42 €/m [32].

3.3.2 Scaling of price with production volume

Because of the used retail prices for materials, cost reductions with higher production volumes need to be implemented. With data from [26], scaling factors for different production volumes can be determined. Assuming a linear influence of production volume X , factors for cost reduction $f_{\text{redu,mat}}$ can be given by:

$$f_{\text{redu,mat}} = k_1 \frac{X}{10^6} + k_2 + 1$$

Kampker [26] gives absolute material costs for steel, aluminum, iron sheets, magnets, copper, insulation, and resin. Based on these costs, relative factors for the mentioned materials can be assumed resulting in the factors k_1 and k_2 Table 6.

Exemplarily, a decrease in the relative material costs of copper from 100% for the lowest possible production volume to 87% at a production volume of 100,000 units/year is notable ($f_{\text{redu,mat}} = 0.87$). The presented linear approach is valid up to a maximum production volume of 150,000 units/year.

3.4 Labor costs

The labor costs in this model base on German average hourly labor costs in the automotive industry of 35.62 €/h [10]. Labor costs include wages and social security contributions. For each production process, the costs for workers that are needed for a manual operation or to supervise the production line $K_{\text{labor},i}$ are implemented by a fixed factor $k_{l,i}$ on the machine runtime T_i .

$$K_{\text{labor},i} = 35.62 \text{€} k_{l,i} T_i$$

For some machines, the factor $k_{l,i}$ is specified in Sect. 3.2, if not, 0.5 is assumed. Additionally, there are purely manual operations performed by the workers. The labor costs incurred by such processes have been described in Sect. 3.2.

In this model, a production based in Germany is assumed. If production happens in countries with lower labor cost levels, some costs can be saved in this category. With average labor cost from eastern European countries of 7 € to 11 € [15], the absolute machine production costs could be reduced. The reduction potential however is limited because labor costs play a minor role regarding the overall costs, with a contribution of only 1.6% to 6.1% to the overall costs (cf. Table 10).

3.5 Purchased parts

Purchased parts comprise the parts that are not manufactured using the previously presented processes but which are typically purchased by suppliers without processing them further (e.g. bearings or resolver). The following non-linear equation is used to estimate its costs K_{purch} .

$$K_{\text{purch}} = X 1229^{-0.284} f_{\text{pow}}$$

Table 6 Parameters of the different materials for the linear cost scaling function

Material	k_1	k_2
Steel	-0.562	5.62e-7
Aluminum	-0.699	6.99e-7
Iron sheets	-0.489	4.89e-7
Magnets	-0.970	9.7e-7
Copper	-1.305	1.31e-6
Insulation	-1.061	1.06e-6
Resin	-1.423	1.42e-6
Average	-0.888	8.88e-7

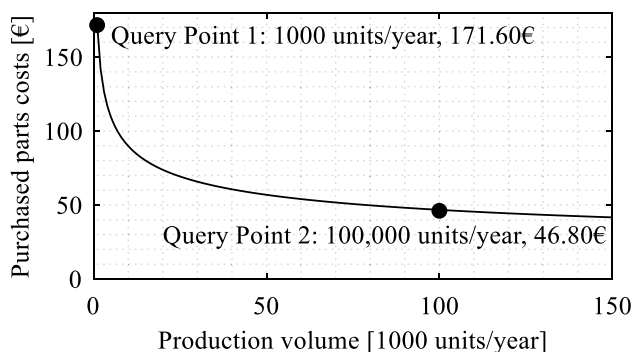


Fig. 3 Function to scale purchased parts costs over production volume for a 50 kW PMSM ($f_{pow} = 1$)

where X is the production volume and f_{pow} is a factor accounting for the influence of rated EM power on costs of the purchased parts. The equation was developed using the following two query points for low and high production volume of a 50 kW PMSM:

1. At a low production volume of 1000 units per year, [25] states overall costs of the purchased parts of 171.60 €.
2. On the other end of production volume range, at 100,000 units per year, [23, 26] states a reduction of the overall purchased parts costs to 46.80 € for the same PMSM.

With above presented equation, a curve results that uses the mentioned query points at low and high production volume (Fig. 3).

Furthermore, a term f_{pow} is introduced in the approximation formula that accounts for the increasing prices of purchased parts with higher machine power (e.g. bigger bearings, more screws, longer cables, etc.).

$$f_{pow} = 1 + 0.5 \frac{P_{nom} - 50kW}{450kW}$$

The equation bases on the assumption that a ten times higher power results in a cost increase of the purchased parts by 50%. The overall costs can be further divided into the individual component’s costs, as listed in Table 7 below.

It is assumed here, that the stated shares of the parts do not change with production volume.

3.6 Final assembly

The costs for the final assembly of the motor K_{ass} are approximated based on data from Kampker [26], who states costs of 77.20 € for a production volume X of 1,000 units per year and 24.28 € for 100,000 units per year. Following equation results from curve fitting:

Table 7 Share of individual purchased part costs of a 50 kW PMSM at production volume of 1,000 units per year [25]

Purchased part	Share from overall costs (%)
Resolver	35.9
Bearings	50.3
Connectors	4.3
Temperature sensors	1.1
Screws	3.1
Other	5.3

$$K_{ass} = X730^{-0.296} f_{pow}$$

Similar as for the purchased parts costs, the factor f_{pow} is introduced to account for an increased assembly effort with more powerful motors.

4 Validation

To validate the correctness of the presented methods, the costs of three selected PMSM were calculated with the presented model and compared to estimations from [33]. Since not all the required cost model input data is publicly available, an FEM model of the motor was developed. By variation of the unknown parameters (e.g., iron sheet material), those parameters with which torque and power rating of the FEM model match the published performance of the real motor could be found out and be used as cost model input. Then, the cost model is executed for multiple production volumes and the production volume at which identical production costs are met is evaluated.

Table 8 shows that the costs for the three PMSM estimated by Munro can be met at realistic production volumes. Overall, the three production volumes are in a range of a series production so that the herein generated cost results are assumed plausible.

Table 8 Cost comparison of series produced EV Motors

Motor	Own cost estimations [€]	Estimations from [33] [€*]
Tesla Model 3 MY2017 (rear)	561.80 at 37,000 units/year	561.64
Chevrolet Bolt	616.17 at 28,600 units/year	616.44
BMW i3	747.58 at 22,800 units/year	747.40

* Based on an exchange rate of 0.9 from USD to EUR.

In [18], 7000 PMSM with different torque and power ratings are analytically laid out and its costs with an assumed production volume of 50,000 units per year are analyzed. In the same torque range as the herein modeled motors (140 Nm to 690 Nm, cf. Fig. 4), the author states production costs of PMSM between 374 € and 1320 €, while our model delivers costs between 353 € and 770 €. The range of herein achieved results is smaller than in the reference and in average cheaper. However, it still lies well within the stated range.

With regards to the comparison of cost values from literature, it is important to mention that the calculation of production costs for reference motors is depending on several unknown aspects. To allow a correct comparison of different costs, basic requirements of all calculations must be the same. Munro for example adds a 22% surcharge for administration, profit, logistics and patent/royalty fees on the raw manufacturing costs [43] which needs to be subtracted since the presented cost model focusses on the production costs without margin. Also from [18], important aspects of his calculations stay unknown such as added margin/profit, raw material price scaling or the exact methods for the generation of EM designs.

With consideration of the natural and described uncertainties, the herein generated results match adequately with the results from [33] and [18]. The presented methods are therefore considered to be realistic.

5 Results

The presented cost model provides the ability to calculate the production costs for a PMSM design for different production volumes. It can additionally be used to vary design parameters (e.g. materials, windings or geometry) to assess their influence on the production costs. In the following, various analyzes are presented, where either the production volume, or the PMSM technology (and associated production processes) are varied and the effect on costs is evaluated.

The estimated absolute costs over the 30 s peak torque specification of 15 typical PMSM in automotive applications for different production volumes are presented in Fig. 4 below.

The cost range is between 306 € and 843 € for a large-scale production and between 1183 € and 1991 € for a small scale production, hence the influence of the production volumes on machine prize is significant. In other words: with a large-scale production, the costs can be reduced up to 77% in comparison to a small scale production. Machines which are relatively big and therefore use a lot of raw materials show less reduction potential with this regards (e.g. BMW i3 motor). It can thus be concluded that the equity, the tooling and the maintenance costs can be reduced much more

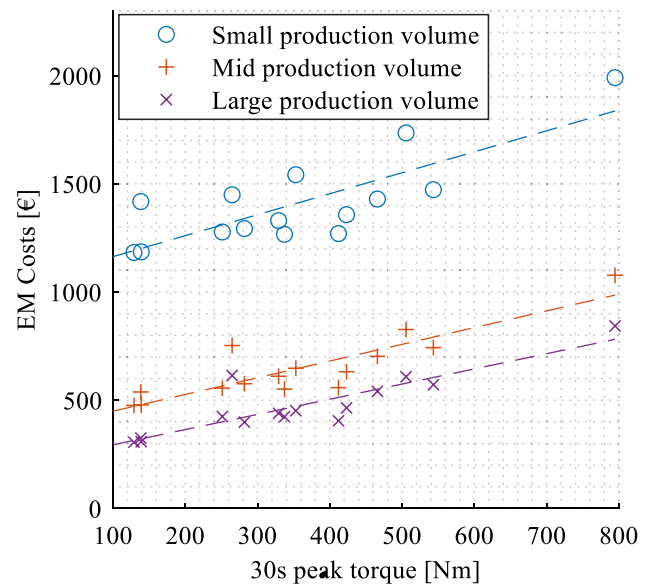


Fig. 4 Costs of various automotive PMSM over torque for different production volumes (“Small production volume” assumes 1000 to 5000 pieces/year, “Medium production volume” 15,000 to 25,000 units/year and “Large production volume 100,000 to 150,000 units/year)”)”)”)

Table 9 Equations for the rough estimation of PMSM production costs based on 30 s peak torque and production volume

Production volume	Equation for cost estimation [€]
Small	$K_{small} = 0.969T_{peak} + 1066$
Medium	$K_{medium} = 0.772T_{peak} + 372$
Large	$K_{high} = 0.701T_{peak} + 224$

over higher production volumes than raw material costs. The linear regression lines in the figure furthermore show that a linear relationship between costs and peak torque rating of the machines can provide a simple approximation. Hence, the following equations can be used to roughly estimate the production costs (in €) of a typical PMSM based solely on its peak torque:

The presented table only provides cost estimation formulae for three different volumes. However, if a more detailed breakdown over production volumes is of interest, Fig. 5 can be referred to.

Figure 5 shows the cost development of a 100 kW/340 Nm motor over the full production volume range. It gets clear, that the cost cannot be decreased linearly with production volume since, as said before, material prices do only decrease to small extend with higher production volumes. This is also confirmed by the following figure, where the cost categories of an exemplary PMSM are displayed:

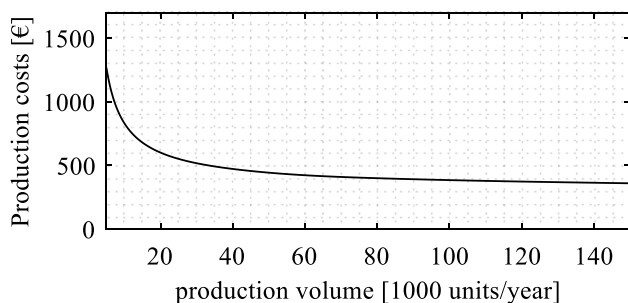


Fig. 5 Production costs of the PMSM design from [20] over production volume

Figure 6 shows how the distribution of the production costs on the different cost categories changes by varying the production volume. The chosen motor for this evaluation is the Tesla Rear PMSM (cf. Table 8). The complete result data is given in Table 10.

For small production volumes the main cost driver is the equity for the machines (depreciation and interest costs), 39% of the EM costs can be attributed to it. Increasing the production volume leads to a higher weighting for the materials as the costs in this category can only be reduced to a small extend with higher volumes. For high production volumes over 100,000 pieces per year, more than half of the costs of a PMSM (58%) can be attributed to the used materials.

The cost model can also be used to evaluate the cost distribution over the different physical parts of the PMSM:

Figure 7 shows a split of the costs among the different parts of the PMSM of four benchmarked motors. The first thing that appears is the high price of the BMWi3 Motor in comparison with the other motors. This is mainly due to its big size in comparison with the other motors and the associated costs for raw materials.

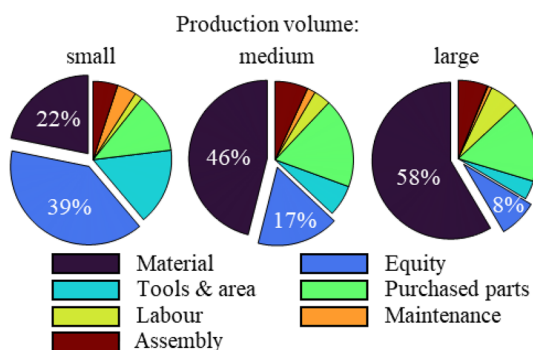


Fig. 6 Share of different cost categories from overall costs for different production volumes

Table 10 Contribution of different cost categories to overall costs for different production volumes

Costs contributions:	Production Volume		
	Small (%)	Medium (%)	Large (%)
Material	21.8	46.1	58.4
Equity	39.3	16.9	8.0
Tools & area	15.8	6.5	3.9
Purchased parts	12.4	18.6	16.6
Labor	1.6	3.5	6.1
Maintenance	4.0	1.7	0.9
Assembly	5.1	6.7	6.1

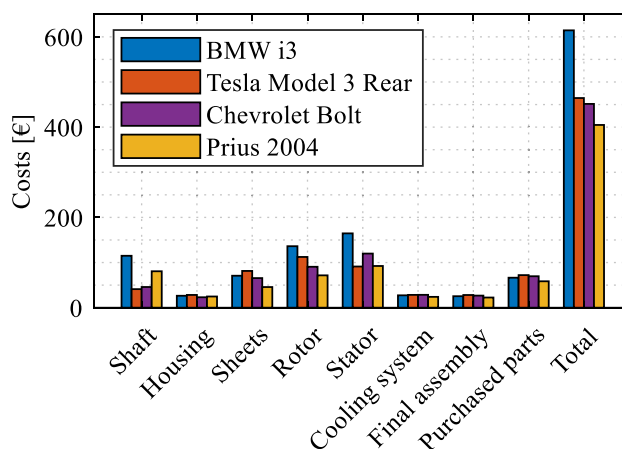


Fig. 7 Costs split over the parts for four benchmarked PMSM (large production volume)

Furthermore, it can be seen from the figure that in this investigation the stator production including its winding is the most cost-intensive part of the PMSM. This is due to complex machinery that is required for the winding and the high resource prices of copper. Magnet assembly (rotor) is the second most expensive part, but it does not, as often postulated, dominate the overall costs alone. Interesting to note is also that housing and cooling system production play (for the herein assumed cooling architectures) only a minor role in comparison to the other parts.

Moreover, the presented cost model enables a systematic comparison of the production costs for different cooling systems:

Figure 8 shows the average costs of the PMSM displayed in Fig. 4, but each of them now modeled with frame or winding cooling system (optionally including rotor cooling), as has been described in Sect. 3.2.6. It can be observed, that a frame cooling represents a cheaper solution than a winding

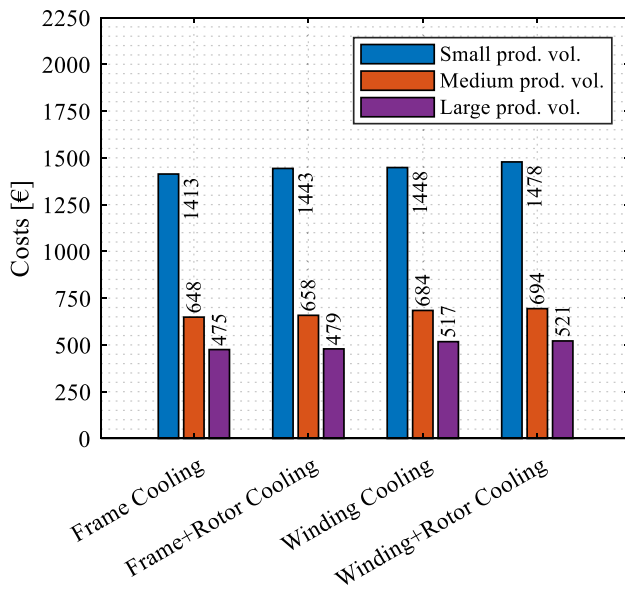


Fig. 8 Average costs of different cooling systems for three production volumes

cooling system: in average over the 15 calculated motors, it is 35 € to 42 € cheaper. The additional costs for the winding cooling system result from the needed end-winding housing and the slot sealing. Additional rotor cooling is in average over the motors only 4€ to 30€ more expensive (depending on production volume) due to its simple assumed geometry (hollow shaft together with some purchased sealings and connectors). In contrast to the winding cooling system production, the additional rotor cooling gets very cheap with high production volumes. This is due to high share of automation, which is assumed for the rotor cooling production, whereas the assumed production processes for the winding cooling system production assume manual work for installing the slot sealing. Furthermore, additional raw materials are being used for the housing, which is not the case for the rotor cooling system.

Next, the costs of different wire technologies are compared. All 15 PMSM designs have been calculated assuming either a round wire winding or hairpin windings. This way, the effect of wire technology on the motors production costs in combination with production volume gets visible (Fig. 9).

Figure 9 shows, that for small production volumes, the hairpin wire technology is more expensive than round wires due to the high investment costs in production machines. On the other hand, the manufacturing process for hairpin wires shows a higher

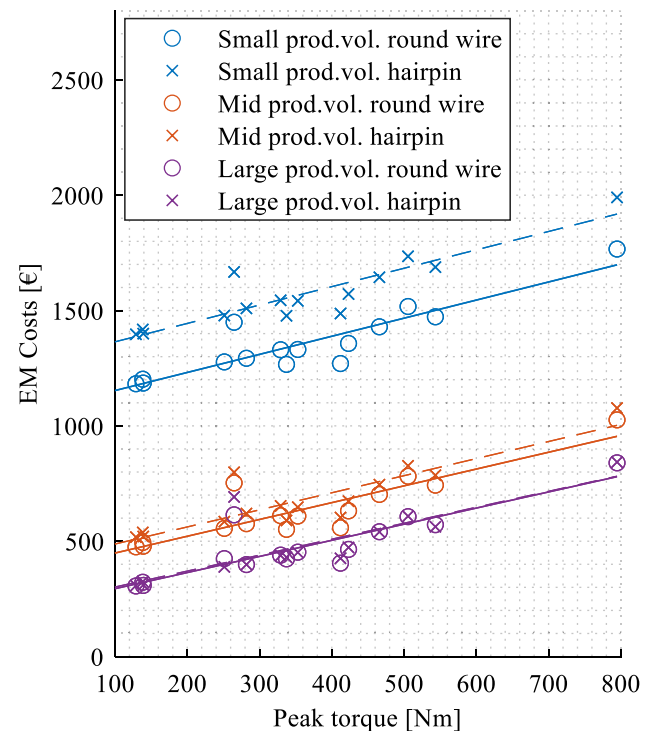


Fig. 9 Costs over torque of PMSM for different production volumes and wire types (round wire and hairpin wire)

grade of automation and therefore less required workers. This leads to the effect, that the costs of hairpin and round wire are almost equal for large-scale production volumes. Hence it can be concluded that the break-even-point, where the hairpin wire production gets cheaper than round wire is just reached here: it lies at a production volume of around 150,000 units/year.

6 Discussion

This chapter intends to outline and discuss the limits of the presented model and investigations: Some of the previously shown results contain findings that were generated by an isolated variation of certain technologies (e.g. winding and cooling system variation). The other motor parameters have not been changed during the variation, so that only the cost aspect of the technology change is visible in the results. It may for instance be that with a more performant cooling system, which is more expensive (here full-winding cooling), the motor can be downsized for same power/torque so that some raw material

costs can be saved. However, considering all these interactions would require a ‘holistic’ approach, implying many iterations of the applied motor designs including computation intensive FEM evaluations. This was not possible to realize within the present research project and hence, interpretation of the generated technology comparison results should be seen under this context. Despite not using a fully ‘holistic’ approach here, we think that the results of an isolated technology variation can serve to better understand the cost implications of different technologies and hence to find better cost-performance compromises in the future.

7 Summary and conclusion

A modular cost model was presented, which delivers valid results. The individual sub-models are interchangeable and can be extended to new finding or adapted to a changing state of the art.

The overall costs for the production of a PMSM are composed from manufacturing, material, labor, assembly and purchased parts costs. Each of those categories shows different characteristics with variation of the production volume. For instance, raw material prices do not get cheaper with the same rate as manufacturing costs with increased production volume. This leads to the effect, that material costs dominate at high production volumes and manufacturing costs at lower production volumes (Fig. 6).

The *machine hour rate calculation* is applied for the estimation of manufacturing costs of PMSM. Here, manufacturing costs are composed of depreciation-, interest-, space-, energy-, maintenance- and tooling costs. All of these costs are evaluated individually for a specific production step and its associated required machines (cf Table 12). By publishing the most important the used methods, scaling functions and assumptions, the herein presented model can be used for further research in this field.

With the calculation of 15 reference motors (six from literature and nine self-designed), a linear relationship can be derived between peak torque of a PMSM and its projected

costs for different production volume (cf. Table 9). The linear relationship is a simplification, but [18] states similar findings.

In general, it was found that the production costs are very sensitive to the assumed production volumes. In average, the cost reduction per motor when ramping up production from 5,000 to 150,000 units/year is 67%.

In another application of the model, the individual parts of the overall costs of the PMSM were assigned to physical parts of the electric motor. It could be shown this way, that the winding (and not as often stated the magnets) seem to present the dominating part of the costs due to its complex production process and the cost of raw copper.

The comparison between the manufacturing costs of round wire and hairpin wire shows that hairpin wires are in most cases the more expensive choice (cf. Fig. 9). However, at an assumed production volume of 150,000 units/year (maximum in this investigation), the costs equalize, reaching the break-even-point: above this volume, hairpin wires are becoming cheaper than round wire technology.

Another conducted technology comparison concerns the cooling system of the PMSM. Herein, a conventional and often seen frame cooling system is compared to the innovative but yet rarely seen direct winding cooling system. In average, the winding cooling system is 39 € more expensive than the frame cooling system, relatively independent from production volume (labor costs are high). An additional simple rotor cooling system is very cheap at high production volumes due to its high grade of automation and only few additional purchased parts: it only adds around 4 € of extra costs. For small production volumes, the difference is greater: up to 30€ extra must be accounted.

The presented cost model makes it possible to evaluate technologies with regards to costs and thus enables a more holistic assessment of technologies for PMSM. This can help in the early development process to identify those designs and materials, which provide the best compromise between costs and performance. Optimizing the cost/performance ratio of electric powertrains will make electric mobility more attractive, thus helping to ramp up registrations, to reduce road transport emissions and to fight climate change a little more.

Table 11 General assumptions of the cost model

Yearly work hours of one employee (T)	1820 h
Working shifts (dynamically adjusted)	1–3
Electricity price k_E [6]	26.64 ct/kWh
Running costs of facility K_{qm} [22]	400 €/m ² /year

Appendix

General Assumptions

The presented cost model makes some general assumptions that apply to all production steps.

See Tables 11, 12.

Table 12 Production machine data

#	Machine Type	Invest [k€]	Depreciation Period [years]	Tool Costs [k€]	Maintenance Cost [k€]	Avg. Power / Energy	Area [m ²]	Reference
1	Die casting	900	6	270	90	40 kW	12	
2	Machining center housing	350	6	105	35	40 kW	12	
3	Deburring	150	5	15	15	40 kW	12	
4	Pressure blasting system	250	5	25	10	40 kW	31	
5	Punch Press	2.000	8	500	200	40 kW	12	[23, 26]
6	Gluing and packaging system	2.700	10	30	270	40 kW	12	[23, 26]
7	Magnet assembly	400	5	40	40	5 kW	12	[37]
8	Slot insulation	200	6	40	20	2.5 kW	12	[37]
9	Impregnation	2.000	6	400	200	10 kW	12	[13, 37]
10	Needle winding	500	6	150	50	11 kW	4.8	[4, 23, 26, 37]
11	Flyer winding	350	6	105	35	11 kW	4.5	[3, 21, 37]
12	Insertion machine	3.800	6	1.140	380	4 kW	12	[18]
13	Laser welding	498	6	50	50	1.42 Wh/ welding	12	[19]
14	Ultrasonic welding	148	6	15	15	1.03 Wh/ welding	12	[19]
15	Bandaging	300	6	60	30	2.5 kW	12	[37]
16	Hairpin production (BM-HP 4500)	2.100	6	210	210	40 kW	12	[35]
17	Hairpin Pre-assembly	800	6	80	80	40 kW	12	[27]
18	Hairpin Basket Assembly	800	6	80	80	40 kW	12	[27]
19	Hairpin Necking	120	6	12	12	40 kW	12	[27]
20	Hairpin Twisting	2.500	6	250	250	40 kW	12	[27]
21	Hydraulic press	2.500	6	625	250	40 kW	12	
22	Lathe	500	5	125	125	40 kW	12	
23	Machining center shaft	700	6	210	70	40 kW	12	
24	Induction heating	1.500	8	150	150	1.68 kW/piece	1.4	[7, 23, 26, 42]

Production machine data

Acknowledgements The presented research was funded by the German Research Foundation (Deutsche Forschungsgemeinschaft – DFG), GRK1856.

Author contributions JH and NN developed the methodology, created the model and wrote the initial draft of the paper together. JH finalized the paper, created the preprint version and managed the review process. NN and LE critically reviewed the paper multiple times and gave valuable feedback. LE supervised the research activity

Funding Open Access funding enabled and organized by Projekt DEAL.

Data availability The generated raw data and files generated during the current study are available from the corresponding author on reasonable request.

Declarations

Conflict of interest The authors have no relevant financial or non-financial interests to disclose.

Open Access This article is licensed under a Creative Commons Attribution 4.0 International License, which permits use, sharing, adaptation, distribution and reproduction in any medium or format, as long as you give appropriate credit to the original author(s) and the source, provide a link to the Creative Commons licence, and indicate if changes were made. The images or other third party material in this article are included in the article's Creative Commons licence, unless indicated otherwise in a credit line to the material. If material is not included in the article's Creative Commons licence and your intended use is not permitted by statutory regulation or exceeds the permitted use, you will need to obtain permission directly from the copyright holder. To view a copy of this licence, visit <http://creativecommons.org/licenses/by/4.0/>.

References

1. AUDI AG.: "Audi Hungaria Startet Serienproduktion Von Elektromotoren." <https://www.audi-mediacycenter.com/de/audimediatv/video/audi-hungaria-startet-serienproduktion-von-elektromotoren-4256> (2018). Accessed 08 Feb. 2022
2. AUDI AG.: "Audi E-Tron Kühlkonzept E-Antrieb (Animation): Animation Zum Kühlkonzept Des E-Antriebs Des Audi E-Tron." <https://www.audi-mediacycenter.com/de/audimediatv/video/audi-e-tron-kuhlkonzept-e-antrieb-animation-4847> (2019). Accessed 21 Feb 2022
3. Aumann, AG.: "Datenblatt Flyerwickelsystem FWS." https://www.aumann.com/fileadmin/images/leistungen/maschinen/Download_Brosch%C3%BCren/Wickeltechnik/Datenblatt_FWS_2019.pdf (2019a).
4. Aumann, AG.: "Datenblatt Nadelwickelsystem NWS." https://www.aumann.com/fileadmin/images/leistungen/maschinen/Download_Brosch%C3%BCren/Wickeltechnik/Datenblatt_NWS_2019.pdf (2019b).
5. Aumann Espelkamp GmbH.: "Nadelwickeln Von Innengenuteten Statoren Auf Einer NWS." <https://www.youtube.com/watch?v=OrJZcJdwoPs> (2016). Accessed 08 Aug 2022
6. BDEW.: "BDEW-Strompreisanalyse Januar 2022: Haushalte Und Industrie." https://www.bdew.de/media/documents/220124_BDEW-Strompreisanalyse_Januar_2022_24.01.2022_final.pdf (2022).
7. Brill, Sascha and Schibisch, Dirk.: "Induktives Härten Versus Einsatzhärten - Ein Vergleich." https://www.sms-elotherm.com/fileadmin/content/PDF/Fachberichte_DE/EW_2014_3_Induktives_H%C3%A4rten_versus_Einsatzh%C3%A4rten_-_ein_Vergleich_Schibisch_Brill.pdf (2014). Accessed 29 July 2022
8. Bubert.: Optimization of electric vehicle drive trains with consideration of parasitic currents inside the electrical machine (2020).
9. Carriero, L., et al.: A review of the state of the art of electric traction motors cooling techniques. In SAE Technical Paper Series. **11**, 435 (2018).
10. Destatis.: "Bruttoverdienste, Wochenarbeitszeit: Deutschland, Quartale, Wirtschaftszweige, Leistungsgruppen, Geschlecht." <https://www-genesis.destatis.de/genesis/online?operation=table&code=62321-0001&levelindex=0&levelid=1648976723731#astructure> (2021). Accessed 03 April 2022
11. Deutsche Börse, AG.: "Aluminium Price." [https://www.boerse-frankfurt.de/commodity/aluminiumpreis\(2022a\)](https://www.boerse-frankfurt.de/commodity/aluminiumpreis(2022a)).
12. Deutsche Börse, AG.: "Copper Price." [https://www.boerse-frankfurt.de/commodity/kupferpreis\(2022b\)](https://www.boerse-frankfurt.de/commodity/kupferpreis(2022b)).
13. Du-Bar, M., et al.: Comparison of performance and manufacturing aspects of an insert winding and a hairpin winding for an automotive machine application. Inter Elect Drives Product Conf. **22**, 1–8 (2018)
14. European Commission.: "European Alternative Fuels Observatory: Vehicles and Fleet European Union." [https://alternative-fuels-observatory.ec.europa.eu/transport-mode/road/european-union-eu27/vehicles-and-fleet\(2021\)](https://alternative-fuels-observatory.ec.europa.eu/transport-mode/road/european-union-eu27/vehicles-and-fleet(2021)). Accessed 28 April 2022
15. Eurostat.: "Hourly Labour Costs: Hourly Labour Costs Ranged Between €7.0 and €46.9 in 2021." [https://ec.europa.eu/eurostat/statistics-explained/index.php?title=Hourly_labour_costs#Hourly_labour_costs_ranged_between_.E2.82.AC7.0_and_.E2.82.AC46.9_in_2021\(2022\)](https://ec.europa.eu/eurostat/statistics-explained/index.php?title=Hourly_labour_costs#Hourly_labour_costs_ranged_between_.E2.82.AC7.0_and_.E2.82.AC46.9_in_2021(2022)).
16. Fernholz.: "Kostenvoranschlag Einsatzstahl 16MnCr5" (2019).
17. Foundation myclimate.: "Climate Booklet: Climate Change and Protection." https://www.myclimate.org/fileadmin/user_upload/myclimate_Klimabooklet_2020_EU.pdf (2020).
18. Fyhr.: Electromobility: Materials and Manufacturing Economics (2018).
19. Gläsel, Tobias.: Prozessketten zum Laserstrahlschweißen von flachleiterbasierten Formspulenwicklungen für automobile Traktionsantriebe (2020).
20. Grunditz.: "Design and assesment of battery electric vehicle powertrain, with respect to performance, energy consumption and electric motor thermal capability. Dissert Chalmers tekniska högskola. **43**, 554 (2016)
21. Hagedorn, J., Blanc, S.-L.: Handbuch der Wickeltechnik für hoch-effiziente Spulen und Motoren: Ein Beitrag zur Energieeffizienz. Springer Vieweg, Berlin, Heidelberg (2016)
22. Hultman, S., et al.: Robotized surface mounting of permanent magnets. Machines **2**(4), 219–232 (2014). <https://doi.org/10.3390/machines2040219>
23. Kampker, D., et al.: Selection of Transformable Production Technologies as a Reaction on a Varying Demand of Electric Traction Motors. Int Elect Drives Prod Conf. **22**, 1–6 (2014)
24. Kampker, D., et al.: Return on engineering: design to cost for electric engine production. Inter Elect Drives Prod Conf. **77**, 1–6 (2015)
25. Kampker.: "Elektromobilkomponentenproduktion." Lecture RWTH Aachen (2021).

26. Kampker, Achim.: *Elektromobilproduktion*. Berlin, Heidelberg: Springer Vieweg (2014)
27. Kampker, Achim, Heimes, Heiner Hans, Kawollek, Sebastian, Treichel, Patrick, Kraus, Andreas, Raßmann Alexander and Hitzel, Tobias.: "Produktionsprozess Eines Hairpin-Stators. https://www.pem.rwth-aachen.de/global/show_document.asp?id=aaaaaahqhgao(2020). Accessed 19 Jan 2022
28. KREMPEL GmbH.: Trivoltherm® Nkn & Trivoltherm® Nk. https://kapman.org/wp-content/uploads/2018/09/TRIVOLTHERM_NKN_TRIVOLTHERM_NK_TDS_KREMPEL_EN_07_2017_2_26.pdf(2017). Accessed 10 Feb 2022
29. Mepa.: "Rundrohr 6x1 Mm, Oberfläche Pressblank Roh. <https://www.mepa-shop.ch/aluprofile/rundrohre/rundrohr-60mmx10mm-pressblank>(2022). Accessed 21 Feb 2022
30. Motointegrator.: "Zusatzwasserpumpe BOSCH 0 392 023 004. https://www.motointegrator.de/artikel/1265900-zusatzwasserpumpe-bosch-0-392-023-004?gclid=Cj0KCQiAt8WOBhDbARIsANQLp95Iqw11BYmSnVPH3-oeYcVyuO4SQXyT5_OrlKB3CV2pq_bB4iHav-waAvZgEALw_wcB (2022). Accessed 04 Feb 2022
31. MPV.: "Silicone Coated Glass Sleeve H Class - GS 40 Type. <https://www.motor-pump-ventilation.com/merchant/product/silicon-coated-glass-sleeve-h-class-gs-40>(2022a). Accessed 10 Feb 2022
32. MPV.: "Trapezoidal Slot Cap NOMEX/POLYESTER/NOMEX. <https://www.motor-pump-ventilation.com/merchant/product/trapezoidal-slot-cap-nomex-polyester-nomex>(2022b). Accessed 04 Aug 2022
33. Munro, Sandy.: "Comparing 10 Leading EV Motors." <https://charge.devs.com/comparing-10-leading-ev-motors/>(2022).
34. Oechslen, Stefan.: *Thermische Modellierung Elektrischer Hochleistungsantriebe*. Wiesbaden: Springer Fachmedien Wiesbaden (2018). Accessed 08 March 2019.
35. Otto Bihler Maschinenfabrik.: E-Mail, 2022, (2022).
36. Plinke, Wulff, Rese, Mario and Utzig, Bernhard Peter.: *Industrielle Kostenrechnung: Eine Einführung*. 8. Auflage. Springer-Lehrbuch. Berlin, Heidelberg: Springer Vieweg (2015).
37. Propfe.: "Marktpotentiale elektrifizierter Fahrzeugkonzepte unter Berücksichtigung von technischen, politischen und ökonomischen Randbedingungen" (2016).
38. Reinap.: "Direct Cooled Laminated Windings" (2015).
39. Reumüller.: "Preisliste 2021/2022. <http://www.reumueller-tewa.at/pdfs/PREISLISTE.pdf>(2022). Accessed 10 Feb 2022
40. Selema, I., et al.: Electrical machines winding technology: latest advancements for transportation electrification. *Machines* **10**(7), 563 (2022). <https://doi.org/10.3390/machines10070563>
41. Sequeira.: "Increasing Electric Machine Power Density with a New End-Winding Cooling System" (2021).
42. SMS Elotherm GmbH.: "ELO-X: Effizient. Zuverlässig. Flexibel. <https://www.sms-elotherm.com/induktives-haerten/universalmaschine/#c9245>(2022). Accessed 29 July 2022
43. Steier, Al and Munday, Alan.: "Advanced Strong Hybrid and Plug-in Hybrid Engineering Evaluation and Cost Analysis" (2017). Accessed 22 July 2022. https://ww2.arb.ca.gov/sites/default/files/2020-04/advanced_strong_hybrid_and_plug_in_hybrid_engineering_evaluation_and_cost_analysis_ac.pdf.
44. Stenzel.: "Großserientaugliche Nadelwickeltechnik für verteilte Wicklungen im Anwendungsfall der E-Traktionsantriebe." Dissertation, Friedrich-Alexander-Universität Erlangen-Nürnberg; Meisenbach KG (2017).
45. Tianjin Ruiyuan Electric Materials Co., Ltd.: "0.4mm * 45 Taped Litz Wire Overall Size 5mm*2mm Profiled Copper Stranded Wire. https://www.alibaba.com/product-detail/0-4mm-45-Taped-Litz-Wire_1600217201803.html?spm=a2700.galleryofferlist.normal_offer.d_title.5e5612d50fLLjf(2022). Accessed 24 Mar 2022
46. Wietschel.: "Ein Update Zur Klimabilanz Von Elektrofahrzeugen" (2020).
47. Zhang, S., et al.: Cost-efficient selection of manufacturing technologies for an electric traction motor shaft produced in China. *Procedia CIRP* **72**, 814–819 (2018). <https://doi.org/10.1016/j.procir.2018.03.206>

Publisher's Note Springer Nature remains neutral with regard to jurisdictional claims in published maps and institutional affiliations.